International Journal of Food Microbiology 292 (2019) 171–183

Contents lists available at ScienceDirect

International Journal of Food Microbiology

journal homepage: www.elsevier.com/locate/ijfoodmicro

# Proteomic analysis of *Saccharomyces cerevisiae* response to plasma treatment

Višnja Stulić[a], Tomislava Vukušić[a,*], Ana Butorac[b], Dean Popović[c], Zoran Herceg[a]

[a] Department of Food Engineering, Faculty of Food Technology and Biotechnology, University of Zagreb, Pierottijeva 6, 10000 Zagreb, Croatia
[b] BioCentre Ltd., Borongajska street 83h, Zagreb, Croatia
[c] Institute of Physics Zagreb, Bijenička street 46, 10000 Zagreb, Croatia

ARTICLE INFO

*Keywords:*
Plasma
*S. cerevisiae*
Yeast cell inactivation
Stress response

ABSTRACT

Food safety is one of the main issues for the food industry. Regarding the increased reports of food-associated infections new non-thermal technologies are rapidly developing and improving. The aim of this research was to define the inactivation, recovery and stress response of *Saccharomyces cerevisiae* ATCC 204508 cells after the treatment by high voltage gas phase plasma and liquid phase plasma discharges in bubbles. Variations of the plasma frequency (60, 90 and 120 Hz), input gas (air or argon) and processing time (5 and 10 min) have been used to define plasma effects on *S. cerevisiae* cells. Complete inactivation's by liquid plasma in bubbles were determined as well as recovery of treated samples. Transmission electron microscopy figures showed cells with the normal cell shape and intact inner and outer membrane after the plasma treatments. Proteomic analyses indicated overexpressed proteins which contributed in cell defense mechanisms to overcome stress conditions. *S. cerevisiae* ATCC 204508 cells were under the stress, but with the proven ability to recover its metabolic activity.

## 1. Introduction

Safe and quality food has become a main issue in a food processing. As a response to mentioned problems new non-thermal technologies are rapidly developing. Pulsed electric field, pulsed light, high voltage electrical discharges, etc. as preservation non-thermal technologies are increasingly used instead of standard pasteurization and sterilization methods. In a past few years high voltage electrical discharges-plasma (HVED) generated in gas or liquid phase has been recognized as non-thermal technique which leads to microorganism's inactivation (Fridman et al., 2007; Sato et al., 1996; Scholtz et al., 2015; Vukusic et al., 2016). Inactivation of undesired microorganisms by HVED depends on several parameters such as the type of microorganism (gram-positive bacteria, gram-negative bacteria, sporogenic bacterial species or yeast cells), the applied treatment (voltage, frequency, power, discharge polarity, reactor configuration) and physical-chemical parameters of the solution (pH, conductivity, temperature, generated free radicals (O·, H·, OH·)) (Liao et al., 2017; Misra et al., 2011; Vukusic et al., 2016).

Despite a considerable amount of the literature that has been published on this topic, there is a question if the microorganisms are lethally injured or just under the stress (sub lethal injury). During the stress conditions (osmotic, acidic, temperature or oxidative stress) cells are activated defending mechanisms to undergo the induced stress which consequently leads to cell recovery. This is a huge problem and threat to human health. Therefore, it is desirable to investigate and define the possible reasons of cell recovery. Furthermore, previous studies have pointed out the differences in microbial inactivation whether it is a prokaryotic or eukaryotic cell (Korachi et al., 2009; Lu et al., 2016; Moreau et al., 2008; Yu et al., 2006). Compared to prokaryotic cell, cell wall of eukaryotic cell is consisted 80–90% of polysaccharides (glucans, mannans and chitin) (Walker, 1998) which complicates their reduction.

This study investigates the influence of gas phase and liquid phase plasma discharges in bubbles on inactivation, recovery and stress response of *S. cerevisiae* ATCC 204508 cells as a function of frequency, treatment time and injected gas (air or argon). Although there are studies on inactivation of different yeast cells, far too little attention has been paid to the recovery and cellular response mechanisms after the HVED treatments. *S. cerevisiae* ATCC 204508 has been chosen as a model organism and one of the most studied yeast organisms. On the other hand, the genome of *S. cerevisiae* has been completely sequenced. Another reason was to investigate inactivation mechanisms and the stress response in a water medium (non-food medium), after which it could be applied to a more complex system of food.

* Corresponding author.
*E-mail address:* tvukusic@pbf.hr (T. Vukušić).

https://doi.org/10.1016/j.ijfoodmicro.2018.12.017
Received 24 July 2018; Received in revised form 13 November 2018; Accepted 19 December 2018
Available online 21 December 2018

## 2. Materials and methods

### 2.1. Design of reactor

For both, gas phase and liquid phase reactor an experimental set-up was consisted of a 1000 mL glass reactor, with a point to plate electrode configuration. In the gas phase, high voltage titanium wire electrode (point) was in the gas phase and the stainless steel grounded electrode (plate, d = 4.5 cm) was in the liquid phase with 0.5 cm electrode distance (Fig. A.1a). Argon (purity 99.99%; Messer, Sulzbach, Germany) or air was injected in the headspace of the reactor at an applied flow of 5 L/min.

For the liquid phase plasma reactor discharges were generated in the bubbles. High voltage electrode (point) was stainless steel medical needle through which argon or air was pumped at an applied flow of 5 L/min. Grounded stainless steel electrode and high voltage electrode were in the liquid phase (Fig. A.1b) with a 1 cm electrode distance.

Electrical circuit was consisted of a capacitor (0.75 nF) which was charged with the pulsed high voltage power supply (Spellman, UK) with a maximum output power of 1200 W and a current of 40 mA to create positive electrical discharges in a gas and liquid phase. Resistors were serially connected with a total resistance of 9.5 MΩ. Frequency was adjusted trough rotary switch-spark-gap. The high voltage probe (Tektronix P6015A) connected to the oscilloscope (Hantek DS05202BM) was used to measure the output voltage (data not shown).

### 2.2. Experimental design

Statgraphics Centurion software (StatPoint Technologies, Inc., VA, USA) was used for the experimental design and statistical analyses (Table 1). Three independent variables were: frequency (Hz) (A), time (min) (B) and gas (air or argon L/h) (C). Statistical calculations were defined using ANOVA at 95% confidence level. A significant level of 0.05 was applied.

### 2.3. Preparation of Saccharomyces cerevisiae ATCC 204508 samples and experimental methods

Samples were prepared by inoculating 10 mL of malt extract broth (Biolife, Milan, Italy) with the 20 µL of the *S. cerevisiae* ATCC 204508. The inoculated malt extract broth was incubated at 30 °C for 48 h without shaking in order of resulting yeast to be in the stationary growth phase. Phase of growth was verified by the optical density measurements at the 600 nm. After the incubation samples were centrifuged (Tehtnica, Centric 150) at 4000 rpm for 10 min at room temperature. Harvested cells were washed three times and re-suspended in the phosphate buffer saline (PBS). After the last centrifugation yeast cells were re-suspended in 0.01 M $NaNO_3$ sterile solution, conductivity of 100 µS/cm. Number of cells before and after the treatment was calculated by the standard dilution method on the malt extract agar (Biolife, Milan, Italy) after the incubation at 30 °C for 48 h and reported as log colony forming units per milliliter ($log_{10}$ CFU/mL).

Treatment volume was composed of the 190 mL of 0.01 M $NaNO_3$, conductivity 100 µS/cm and 10 mL of *S. cerevisiae* ATCC 204508 suspension. The initial pH was 7.00 ± 0.05 and the samples were treated for 5 and 10 min. Conductivity and pH of the samples were measured before and after the treatment using a pH and conductivity meter (HI-2030-edge, Hanna Instruments). The initial temperature was around 18 °C (Tables 2 and 3). The temperature was measured using an infrared thermometer (PCE-777, PCE Instruments). Concentration of generating extracellular $H_2O_2$ was measured spectrophotometrically (ECOMAM UviLine 9400 Spectrophotometer, Secomam Groupe Aqualabo, France) at the 410 nm with the addition of 2 mL of sample and 1 mL of the titanium sulphate (Eisenberg, 1943). Unless otherwise stated, all experiments were analyzed three times (as the repetition of three experiments) and the final results are the mean values of three determinations.

**Table 1**
Experimental design for the treatment time, frequency and gas.

| Sample | Time (min) | Frequency (Hz) | Gas[a] |
|---|---|---|---|
| 1 | 10 | 90 | 0 |
| 2 | 5 | 60 | 1 |
| 3 | 5 | 120 | 0 |
| 4 | 5 | 90 | 1 |
| 5 | 5 | 90 | 0 |
| 6 | 5 | 120 | 1 |
| 7 | 10 | 90 | 1 |
| 8 | 10 | 60 | 0 |
| 9 | 5 | 60 | 0 |
| 10 | 10 | 60 | 1 |
| 11 | 10 | 120 | 1 |
| 12 | 10 | 120 | 0 |

[a] 0 = air; 1 = argon.

**Table 2**
Analysis of variance for the inactivation effect on *S. cerevisiae* ATCC 204508 cells after gas phase plasma treatment ([a]) and liquid phase plasma discharges in bubbles ([b]). Statistical significance $p < 0.05$.

| | Reduction[a] ($log_{10}$ CFU/mL) | | Reduction[b] ($log_{10}$ CFU/mL) | |
|---|---|---|---|---|
| Source* | F ratio | p-Value | F ratio | p-Value |
| A | 0.56 | 0.4963 | 0.27 | 0.6325 |
| B | 0.07 | 0.7978 | 874.01 | 0.0000 |
| C | 1.55 | 0.2815 | 917.32 | 0.0000 |
| A:A | 0.13 | 0.7322 | 15.72 | 0.0166 |
| A:B | 0.06 | 0.8188 | 0.66 | 0.4622 |
| A:C | 2.43 | 0.1942 | 0.38 | 0.5716 |
| B:C | 2.43 | 0.05 | 0.38 | 399.89 |

* A - frequency, B - time, C - gas, A:A - quadratic effect of frequency, A:B - combined effect of frequency (A) and time (B), A:C - combined effect of frequency (A) and gas (C), B:C - combined effect of time (B) and gas (C).

### 2.4. Optical emission spectroscopy

Optical emission spectroscopy was performed using spectrometer Avantes AvaSpec 3648 in the range from 200 to 1100 nm with a nominal spectral resolution of 0.8 nm. With a quartz lens, which was attached to optical fiber the light from the discharge region was collected. For each measurement, approximately 30 spectra were recorded and then averaged. Optical signal integration time was set to 500 ms, which corresponds to 1350 recorded discharges (at 90 Hz gas discharge frequency in argon) per measurement.

### 2.5. Recovery of treated samples

Recovery test was conducted after the one-time treatment. Recovered cells present the cells which had an ability to continue its metabolic activity after the treatment by HVED. Sample volume of 1 mL was added to 9 mL of malt extract broth (Biolife, Milan, Italy) and incubated at the 30 °C for 48 h. The number of cells was calculated by the standard dilution method on malt extract agar (Biolife, Milan, Italy). The results were reported as log colony forming units per milliliter ($log_{10}$ CFU/mL).

### 2.6. Transmission electron microscopy (TEM)

The yeast cells were collected for the transmission electron microscopy by centrifugation (Rotina 380R, Germany) before and after the treatment (liquid phase plasma discharges in bubbles, 90 Hz, 10 min,

**Table 3**
Physical-chemical results for the concentration of extracellular $H_2O_2$ (mg/L), pH, conductivity (μS/cm) and temperature (°C) before and after the gas phase plasma treatment. All values are expressed as a three independent experiments ± standard deviation.

| Sample | $H_2O_2$ (mg/L)[a] | $H_2O_2$ (mg/L)[b] | pH[a] | pH[b] | σ (μS/cm)[a] | σ (μS/cm)[b] | T (°C)[a] | T (°C)[b] |
|---|---|---|---|---|---|---|---|---|
| 1 | 0.103 ± 0.01 | 10.11 ± 0.05 | 7.05 ± 0.05 | 4.21 ± 0.02 | 100.4 ± 0.02 | 145.2 ± 0.05 | 18.4 ± 0.001 | 25.4 ± 0.005 |
| 2 | 0.206 ± 0.05 | 6.42 ± 0.02 | 6.88 ± 0.02 | 4.89 ± 0.02 | 100.0 ± 0.01 | 141.8 ± 0.05 | 18.0 ± 0.008 | 24.9 ± 0.005 |
| 3 | 0.103 ± 0.02 | 8.75 ± 0.01 | 7.00 ± 0.02 | 6.23 ± 0.05 | 100.2 ± 0.01 | 112.4 ± 0.01 | 18.2 ± 0.005 | 21.4 ± 0.002 |
| 4 | 0.308 ± 0.02 | 6.78 ± 0.01 | 7.00 ± 0.05 | 6.03 ± 0.05 | 100.1 ± 0.01 | 129.6 ± 0.01 | 18,0 ± 0.005 | 24.7 ± 0.002 |
| 5 | 0.308 ± 0.01 | 10.99 ± 0.01 | 7.00 ± 0.05 | 5.12 ± 0.04 | 100.1 ± 0.05 | 168.4 ± 0.02 | 18.0 ± 0.001 | 28.7 ± 0.005 |
| 6 | 0.103 ± 0.01 | 5.36 ± 0.04 | 6.99 ± 0.01 | 6.21 ± 0.05 | 100.0 ± 0.05 | 110.7 ± 0.02 | 18.2 ± 0.001 | 20.8 ± 0.005 |
| 7 | 0.103 ± 0.05 | 4.27 ± 0.01 | 6.99 ± 0.01 | 5.87 ± 0.01 | 100.0 ± 0.05 | 117.6 ± 0.05 | 18.2 ± 0.003 | 22.4 ± 0.003 |
| 8 | 0.103 ± 0.01 | 5.25 ± 0.05 | 7.05 ± 0.05 | 5.11 ± 0.01 | 100.4 ± 0.04 | 127.6 ± 0.05 | 18.4 ± 0.003 | 22.3 ± 0.001 |
| 9 | 0.206 ± 0.01 | 5.15 ± 0.05 | 6.88 ± 0.05 | 5.29 ± 0.04 | 100.0 ± 0.05 | 124.3 ± 0.02 | 18.0 ± 0.001 | 22.0 ± 0.001 |
| 10 | 0.103 ± 0.02 | 12.23 ± 0.03 | 7.00 ± 0.02 | 5.36 ± 0.05 | 100.0 ± 0.05 | 163.8 ± 0.02 | 18.0 ± 0.001 | 28.4 ± 0.003 |
| 11 | 0.103 ± 0.01 | 10.21 ± 0.03 | 7.00 ± 0.02 | 5.07 ± 0.05 | 100.2 ± 0.02 | 126.2 ± 0.05 | 18.2 ± 0.005 | 21.7 ± 0.003 |
| 12 | 0.103 ± 0.01 | 8.56 ± 0.01 | 7.00 ± 0.02 | 5.48 ± 0.01 | 100.0 ± 0.02 | 140.0 ± 0.05 | 18.0 ± 0.005 | 24.3 ± 0.003 |

[a] Before treatment.
[b] After the treatment.

argon) at 9000 rpm for 10 min. The concentration of the analyzed cells was $10^6$ CFU/mL before and after the treatment. Fixation was done on the ice and the cells were washed with Na-cac buffer solution (0.05 M). After that, centrifugation at the 3000 rpm for 5 min was done. Furthermore, 2% glutaraldehyde dissolved in a Na-cac buffer (0.05 M) at the pH 7.2 was added to the cells for 20 min and after that sample was centrifuged at the 3000 rpm for 5 min. Likewise, 2% glutaraldehyde dissolved in a Na-cac buffer (0.05 M) at the pH 7.2 for 40 min was added. The suspension was washed four times with a Na-cac buffer solution (0.05 M) for 10 min. Post fixation was done with a 2% osmium-tetroxide dissolved in a Na-cac buffer (0.05 M) at the pH 7.2 for 1 h and centrifuged at the 3000 rpm for 5 min. Sample was washed four times with deionized $H_2O$ for 10 min. Dehydration was done with the ethanol solutions starting with the 50%, 60%, 70%, 80% and 90% for 10 min. After that absolute ethanol (Kemika, Zagreb, Croatia) was left overnight. Next day suspension was centrifuged at the 3000 rpm for 5 min and absolute ethanol: acetone 1:1 was added to the cells for 1 h. Suspension was centrifuged at the 3000 rpm for 5 min. The next step was the addition of acetone (Kemika, Zagreb, Croatia) for 1 h followed by centrifugation at the 3000 rpm for 5 min. Infiltration was done in a shaker. Spurr resin:acetone mixture 1:2 was added for 1 h. After that spurr resin:acetone mixture 1:1 was added for 2 h and mixture of spurr resin:acetone 2:1 for 3 h. Through the night 100% spurr resin was added to the cells in a shaker. The polymerization was done in Eppendorf tubes for 48 h at the 65 °C. Cutting of the ultrathin sections (60–70 μm) was done with the ultramicrotome (Leica Ultracut R). Contrasting was done with the addition of the 2% uranyl acetate for 10 min. Suspension was washed with the deionized $H_2O$ for 10 min. Lead citrate was added for 10 min and washed with warm deionized $H_2O$ for 10 min. Microscoping was conducted with the transmission electron microscope (Zeiss EM 10). All chemicals were purchased from Sigma Aldrich Co., Munich, Germany unless otherwise indicated.

### 2.7. Quantitative analysis of proteins

Liquid phase plasma discharges in bubbles with a treatment parameters of 90 Hz, 10 min and injected gas argon has been selected for the proteomic analyses, due to the best inactivation results. In order to better understand inactivation mechanism through proteomic response, *S. cerevisiae* cells were treated once and three times at frequency of 90 Hz, 10 min and injected gas argon. Quantitative analyses of proteins were done in duplicate using the ESI-qTOF SYNAPT G2-Si (Waters, USA) of a treated and recovered *S. cerevisiae* cells. Preparation of samples followed the procedure as described in (Preparation of *Saccharomyces cerevisiae* ATCC 204508 Sample and Experimental Methods). Sample which was under the one-time treatment was prepared by adding 20 μL of the *S. cerevisiae* cells into the 10 mL of malt extract broth and incubated for 48 h at 30 °C. After the one-time treatment 20 μL of treated sample was inoculated into the 10 mL of malt extract broth and incubated for 48 h at 30 °C. This sample presented recovery sample. For three time treated sample, first 20 μL of the *S. cerevisiae* cells into the 10 mL of malt extract broth was inoculated and incubated at 30 °C for 48 h. After the first treatment again 20 μL of one-time treated sample was inoculated into the 10 mL of malt extract broth and incubated for 48 h at 30 °C. This was a sample for the second treatment. After the second treatment 20 μL of the second-treated sample was inoculated into the 10 mL malt extract broth and incubated for 48 h at 30 °C. This was a sample for the third treatment. To collect cells after the treatments and recovery test, yeast cells were harvested at 9000 rpm (Tehtnica, Centric 150) for 10 min. The cells were washed twice in PBS buffer. Proteins were isolated as described in the protocol Pierce™ Mass Spec Sample Prep Kit for Cultured Cells with a simple modification in lysis step. Briefly, lysis was done by adding five cell-pellet volumes of the lysis buffer and one cell-pellet volume of glass beads (0.4 mm in diameter) and vortexed for 3 min. Samples were harvested at the 10,000 rpm and 8 °C after the cells lysis. A Bradford method with a NanoDrop One/Onec, UV–Vis Spectrophotometer (Thermo Scientific, USA) was used to define the concentration of proteins. Four volumes of acetone cooled to −20 °C were added to the 50 μg of proteins. Furthermore, the samples were incubated for 2 h at −20 °C and proteins were harvested at 10000 rpm for 10 min at 8 °C. Collected proteins were dissolved in 50 μL of the digestion buffer according to the protocol Pierce™ Mass Spec Sample Prep Kit for Cultured Cells. BSA protein was spiked into each sample as a reference protein for relative quantification. The stock solution of BSA was prepared in digestion buffer (Pierce™ Mass Spec Sample Prep Kit for Cultured Cells), the concentration was adjusted to 0.5 mg/mL and confirmed by using NanoDrop One/Onec, UV–Vis Spectrophotometer (Thermo Scientific, USA). Solubilized BSA was spiked into each sample after adjusting total protein content. The spiked BSA amount was set to 0.5% of total protein amount. The trypsin proteolysis was performed according to the manufacturer's instructions (trypsin from porcine pancreas; Merck, Germany). Following digestion, the extracted peptides were purified and separated in the NanoAcquity UPLC system (Waters, USA). For the purification 2G-V/M Trap 5 μm Symmetry C18, 180 μm × 20 mm (Waters, USA) pre-column was used with a flow rate of 15 μL/min.

Acquity UPLC column BEH300 C18, 100 μm × 100 mm (Waters, USA) was used for separation of peptides with a gradient solvent A (0.1% formic acid in $H_2O$) and solvent B (95% acetonitrile, 0.1% formic acid in $H_2O$) at a flow rate of 1 μL/min. Mass spectrometry was performed using an ESI-qTOF SYNAPT G2-Si (resolution mode of operation) mass spectrometer (Waters, USA). The instrument parameters were set using the Mass Lynx software version 4.1. SCN902 (Waters, USA). LC–MS data were collected in low energy and elevated energy

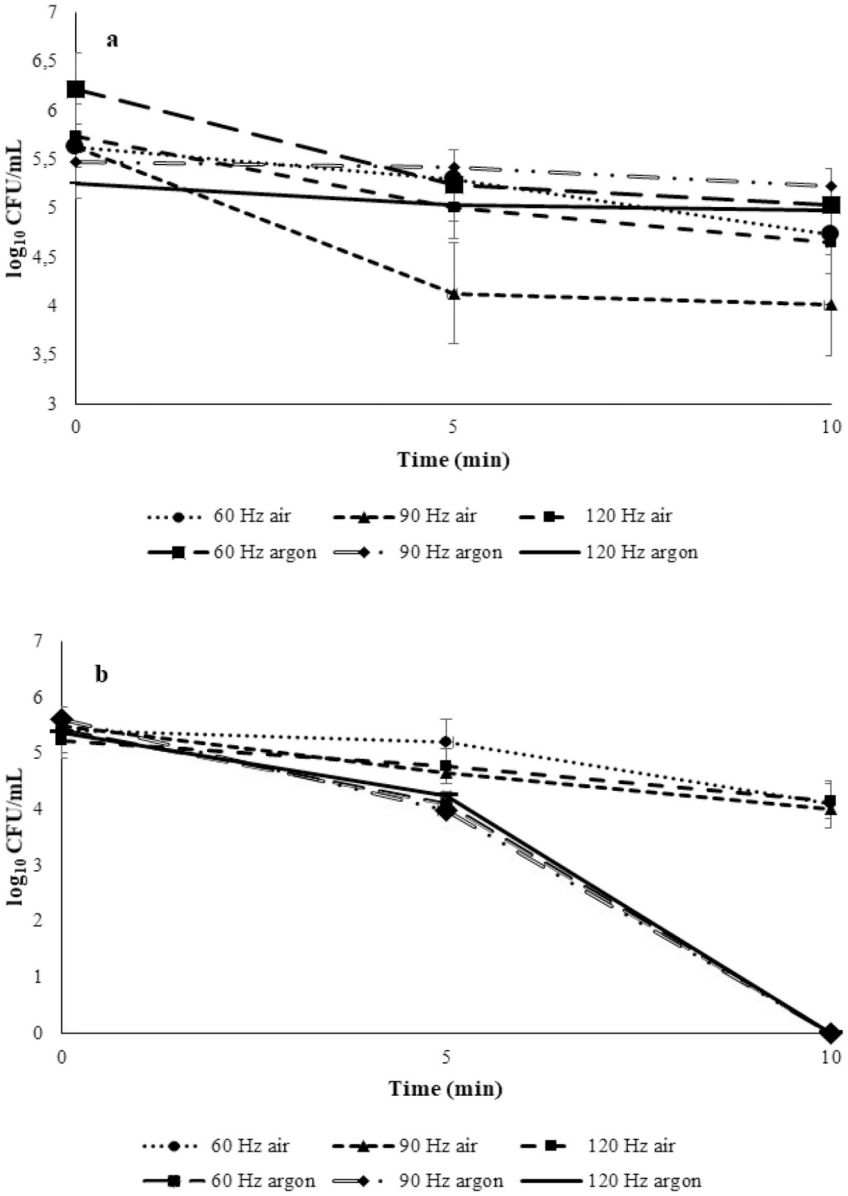


**Fig. 2.** The effect of frequency, time and injected gas on inactivation of *S. cerevisiae* ATCC 204508 by gas phase plasma treatment (a) and liquid phase plasma generated in bubbles (b).

($MS^E$) mode of acquisition. Acquisitions were performed in the positive ion reflectron mode and desolvation nitrogen flow of 0.6 bar at 150 °C. Capillary voltage was 4 kV. Cone voltage was 40 V. In low energy MS mode, data were collected at constant collision energy of 4 eV and in elevated energy MS mode the collision energy was ramped from 20 to 45 eV during each 1 s data collection cycle. Mass spectra were obtained in a mass range *m/z* 700–4000. Leucine-enkephalin 1 ng/μL was used as internal calibration of the mass range (0.3 μL/min, *m/z* 556.2771 Da $[M + H]^+$). Three technical replicates per biological sample were analyzed. Identification of proteins was performed by a ProteinLynx Global Server 3.0.1. (Waters, USA). The raw data were processed and the peak lists were generated after deisotoping and deconvolution. Processed spectra were searched against the complete proteome set of *S. cerevisiae* from UniProt (release 2017_3). The detection limit was 125 counts with a fragment tolerance of 0.25 Da. Relative label-free quantification was done in PLGS software by Expression Analysis tool, all three technical replicates, and both biological replicates were included in the analysis. An internal standard method (using spiked BSA peptides) was employed for normalization. Probability of up or downregulation was ≥95%. Only peptides designated by PLGS as OK were included in protein quantification. Control was non-treated sample. Fold change cutoff was > 1.5 (Oberg and Vitek, 2009). All chemicals and materials were purchased from Merck, Germany.

## 3. Results

### 3.1. Inactivation of S. cerevisiae ATCC 204508 cells and physical-chemical results

The inactivation results yielded by this study provide convincing evidence that there is a significant difference among liquid phase plasma discharges in bubbles and gas phase plasma treatments. The effect of gas phase plasma generated in the air and argon didn't show a significant reduction in *S. cerevisiae* ATCC 204508 cells (Fig. 2a), regardless of the applied treatment time, gas and the frequency. The highest reduction (1.59 $\log_{10}$ CFU/mL) after the gas phase plasma treatment was obtained after the 10 min, 90 Hz and injected gas, air. A closer look at the data shown in the Fig. 2a indicates that at the

**Table 4**
Physical-chemical results for the concentration of extracellular $H_2O_2$ (mg/L), pH, conductivity (μS/cm) and temperature (°C) before and after the treatment by liquid phase plasma discharges in bubbles. All values are expressed as a three independent experiments ± standard deviation.

| Sample | $H_2O_2$ (mg/L)[a] | $H_2O_2$ (mg/L)[b] | pH[a] | pH[b] | σ (μS/cm)[a] | σ (μS/cm)[b] | T (°C)[a] | T (°C)[b] |
|---|---|---|---|---|---|---|---|---|
| 1 | 0.206 ± 0.05 | 5.44 ± 0.02 | 7.00 ± 0.01 | 4.75 ± 0.05 | 100.1 ± 0.04 | 148.4 ± 0.05 | 18.1 ± 0.001 | 26.1 ± 0.002 |
| 2 | 0.401 ± 0.04 | 3.33 ± 0.02 | 6.98 ± 0.05 | 4.82 ± 0.05 | 100.0 ± 0.04 | 137.1 ± 0.05 | 18.0 ± 0.005 | 25.1 ± 0.007 |
| 3 | 0.103 ± 0.04 | 6.9 ± 0.05 | 7.00 ± 0.05 | 5.99 ± 0.02 | 100.0 ± 0.05 | 114.1 ± 0.02 | 18.1 ± 0.009 | 19.9 ± 0.002 |
| 4 | 0.103 ± 0.05 | 4.11 ± 0.05 | 6.98 ± 0.05 | 6.01 ± 0.01 | 100.0 ± 0.05 | 142.7 ± 0.04 | 18.1 ± 0.009 | 25.8 ± 0.002 |
| 5 | 0.103 ± 0.05 | 9.32 ± 0.05 | 6.98 ± 0.01 | 4.75 ± 0.01 | 100.0 ± 0.05 | 174.3 ± 0.05 | 18.1 ± 0.001 | 29.7 ± 0.001 |
| 6 | 0.103 ± 0.02 | 2.82 ± 0.03 | 7.01 ± 0.02 | 6.24 ± 0.05 | 100.0 ± 0.03 | 112.5 ± 0.05 | 18.0 ± 0.001 | 20.1 ± 0.005 |
| 7 | 0.103 ± 0.02 | 3.6 ± 0.03 | 7.01 ± 0.02 | 5.14 ± 0.05 | 100.0 ± 0.02 | 124.1 ± 0.03 | 18.0 ± 0.001 | 22.3 ± 0.001 |
| 8 | 0.206 ± 0.05 | 4.18 ± 0.04 | 7,00 ± 0.01 | 6.11 ± 0.01 | 100.1 ± 0.05 | 136.4 ± 0.05 | 18.1 ± 0.005 | 24.2 ± 0.001 |
| 9 | 0.401 ± 0.05 | 2.72 ± 0.05 | 6.98 ± 0.01 | 6.14 ± 0.01 | 100.0 ± 0.05 | 127.1 ± 0.05 | 18.0 ± 0.001 | 21.8 ± 0.005 |
| 10 | 0.206 ± 0.01 | 9.36 ± 0.05 | 7.00 ± 0.02 | 4.25 ± 0.03 | 100.0 ± 0.05 | 168.6 ± 0.02 | 18.2 ± 0.005 | 28.8 ± 0.005 |
| 11 | 0.103 ± 0.01 | 8.46 ± 0.05 | 7.00 ± 0.01 | 5.02 ± 0.03 | 100.0 ± 0.02 | 120.3 ± 0.02 | 18.1 ± 0.005 | 21.4 ± 0.001 |
| 12 | 0.206 ± 0.05 | 5.11 ± 0.01 | 7.00 ± 0.01 | 5.24 ± 0.01 | 100.0 ± 0.02 | 135.9 ± 0.02 | 18.2 ± 0.001 | 24.4 ± 0.001 |

[a] Before treatment.
[b] After the treatment.

frequencies of 60 and 120 Hz after the 10 min of treatment and injected gas, air, only 0.9 $\log_{10}$ CFU/mL and 1.09 $\log_{10}$ CFU/mL reductions were achieved. With the applied gas argon, the highest reduction of 1.18 $\log_{10}$ CFU/mL after the 60 Hz and 10 min was noted (Fig. 2a).

Contrary to gas plasma, application of liquid plasma discharge in bubbles after 10 min of treatment at the frequencies of 60, 90 and 120 Hz with the applied gas argon resulted in complete inactivation of *S. cerevisiae* ATCC 204508 (cells were reduced to undetectable levels) as shown in the Fig. 2b. The most effective inactivation of 5.61 $\log_{10}$ CFU/mL was achieved at the frequency of 90 Hz. In experiments with the air as working gas, the highest reduction of 1.47 $\log_{10}$ CFU/mL was also observed after the treatment of 90 Hz and 10 min (Fig. 2b). From the presented data it can be observed that influence of treatment time and injected gas (air or argon), highly affected the inactivation results. The statistical influence of treatment factors on inactivation data were carried out by the response surface methodology (RSM) using a Statgraphics Centurion software. According to the Table 2 none of the factors had a statistically significant influence on the inactivation of *S. cerevisiae* ATCC 204508 for the treatment of gas phase plasma ($p > 0.05$), but for the liquid phase plasma discharges in bubbles significant influence ($p < 0.05$) was observed for variables of time (B), gas (C) and quadratic effect of the frequency (A:A).

Physical-chemical results are presented in Tables 3 and 4. The highest concentration of extracellular $H_2O_2$ species, 12.01 mg/L was obtained after the gas phase plasma treatment (10 min of treatment, 60 Hz, argon) which correlates with the high inactivation rate (1.18 $\log_{10}$ CFU/mL) after the same treatment. In the gas phase reactor ions, radicals and neutral species can transfer into the liquid phase by the action of an electric field (Locke et al., 2006, p.894). $H_2O^+$ ions which are formed during the gas phase treatment are bombarding the gas-liquid interface causing the formation of OH· radicals, which can recombine and form hydrogen peroxide (Locke et al., 2006, p.894). Chemistry of liquid discharges in bubbles is similar to gas phase discharges while plasma is generated in the gas and liquid phase. According to Table 5 statistically significant effect ($p < 0.05$) on the concentration of extracellular $H_2O_2$ at the gas phase reactor had frequency (A), time (B) and gas (C). For the liquid phase plasma discharges in bubbles significant influence ($p < 0.05$) on the concentration of extracellular $H_2O_2$ had time (B), gas (C), quadratic effect of frequency (A:A), combined effect of frequency and time (A:B) and combined effect of frequency and gas (A:C).

The lowest pH (4.21 ± 0.02) was also obtained after the gas phase plasma treatment, but at the treatment regime of 90 Hz, 10 min and input gas air. As the temperature increased, proportionally conductivity was higher. The temperature increased in all experiments, but higher increase occurred in the treatments at higher frequencies. The highest measured temperature (29.7 ± 0.001) suggests the non-thermal nature of plasma treatment, still not sufficient for significant inactivation of *S. cerevisiae* ATCC 204508. According to Table 5 statistically significant effect ($p < 0.05$) on the pH at the gas phase reactor had time (B) and quadratic effect of frequency (A:A), on the temperature statistically significant effect had frequency (A), time (B) and combined effect of frequency and time (A:B) and for the conductivity statistically significant effect at the gas phase reactor had frequency (A), time (B) and combined effect of frequency and time (A:B). For the liquid phase plasma discharges in bubbles significant influence ($p < 0.05$) on pH had frequency (A), time (B) and gas (C) and on the temperature and conductivity statistically significant effect had frequency (A) and time (B). The increment in temperature during the plasma treatments is due to elastic and non-elastic collisions of electrons and molecules (Inagaki, 1996). According to the expression /1/ increment in frequency consequently induces higher discharge power. During the discharges at the

**Table 5**
Analysis of variance for the effect of concentration of extracellular $H_2O_2$, pH, conductivity and temperature on *S. cerevisiae* ATCC 204508 cells after gas phase plasma treatment ([a]) and liquid phase plasma discharges in bubbles ([b]). Statistical significance $p < 0.05$.

| Source* | $H_2O_2$[a] (mg/L) | | $H_2O_2$[b] (mg/L) | | pH[a] | | pH[b] | | σ[a] (μS/cm) | | σ[b] (μS/cm) | | T (°C)[a] | | T (°C)[b] | |
|---|---|---|---|---|---|---|---|---|---|---|---|---|---|---|---|---|
| | F ratio | p-Value | F ratio | p-Value | F ratio | p-Value | F ratio | p-Value | F ratio | p-Value | F ratio | p-Value | F ratio | p-Value | F ratio | p-Value |
| A | 11,64 | 0,02 | 5,73 | 0,07 | 2,30 | 0,20 | 15,85 | 0,01 | 93,31 | 0,00 | 56,97 | 0,00 | 389,32 | 0,00 | 61,71 | 0,00 |
| B | 17,56 | 0,01 | 21,03 | 0,01 | 11,30 | 0,02 | 119,69 | 0,00 | 75,69 | 0,00 | 18,18 | 0,01 | 156,57 | 0,00 | 20,11 | 0,01 |
| C | 23,85 | 0,00 | 21,23 | 0,01 | 4,11 | 0,11 | 7,91 | 0,04 | 0,54 | 0,51 | 0,06 | 0,82 | 0,39 | 0,56 | 0,02 | 0,88 |
| A:A | 7,50 | 0,05 | 20,40 | 0,01 | 14,38 | 0,01 | 1,37 | 0,30 | 0,96 | 0,39 | 0,02 | 0,89 | 4,89 | 0,09 | 0,20 | 0,68 |
| A:B | 7,19 | 0,05 | 8,31 | 0,04 | 0,26 | 0,64 | 0,12 | 0,74 | 16,80 | 0,02 | 5,44 | 0,08 | 35,27 | 0,00 | 2,16 | 0,21 |
| A:C | 4,44 | 0,10 | 10,77 | 0,03 | 0,28 | 0,62 | 3,38 | 0,14 | 1,32 | 0,33 | 0,27 | 0,63 | 0,33 | 0,59 | 0,15 | 0,72 |
| B:C | 2,66 | 0,17 | 0,05 | 0,83 | 0,22 | 0,66 | 0,32 | 0,60 | 0,04 | 0,86 | 0,01 | 0,92 | 0,61 | 0,47 | 0,17 | 0,69 |

* A - frequency, B - time, C - gas, A:A - quadratic effect of frequency, A:B - combined effect of frequency (A) and time (B), A:C - combined effect of frequency (A) and gas (C), B:C - combined effect of time (B) and gas (C).

positive polarity higher frequency and discharge power influenced the strong photoionization effect where the energy was transferred to the surrounding medium and consequently warmed it.

$$P = \frac{1}{2} xCxU^2xf \quad (1)$$

### 3.2. Optical emission spectroscopy results

Optical emission spectroscopy is here primarily used for the identification of different excited species present in the discharge region (shown in the Fig. 4 in case of 100 µS conductivity, positive polarity and gas phase discharge in argon). One can see the argon and titanium neutral and ionic lines as the hydrogen and oxygen atomic lines. Interestingly presence of neutral and ionized titanium lines is a sign of unwanted erosion of the titanium electrode placed above the water surface. While $OH^-$ band is not resolved in the spectrum due to its overlap with titanium ionic lines, the $OH^-$ radical is most certainly created in the discharge by water dissociation, which is supported with observed hydrogen (656 nm) and oxygen (777 nm) atomic lines. Other than plasma composition, electron density was determined (Griem, 1974) by measuring the full width at half maximum (FWHM) of Stark broadened hydrogen-alpha (656 nm) line and assuming the electron temperature of 1 eV. In our case, FWHM equals 1.65 nm leads to electron number density of $7.5 \times 10^{16}$ cm$^{-3}$.

### 3.3. Recovery test results

In a relation of inactivation results, cell recovery analyses were conducted. Recovery of microbial cells gives very important insight weather the cells are dead or sub-lethally injured after the treatment. Fig. 3 shows important recovery results of *S. cerevisiae* ATCC 204508 cells after the liquid plasma discharges in bubbles at the treatment regime of 60, 90 and 120 Hz, 10 min and injected gas argon. After the treatments, samples were placed into the optimum conditions (temperature, nutrient medium, pH) and $\log_{10}$ CFU/mL were counted. Overall, it is important to note that complete inactivation's of yeast cells were achieved, but at the end treated cells recovered their metabolic activity. This result implies stress condition of the *S. cerevisiae* ATCC 204508 cells.

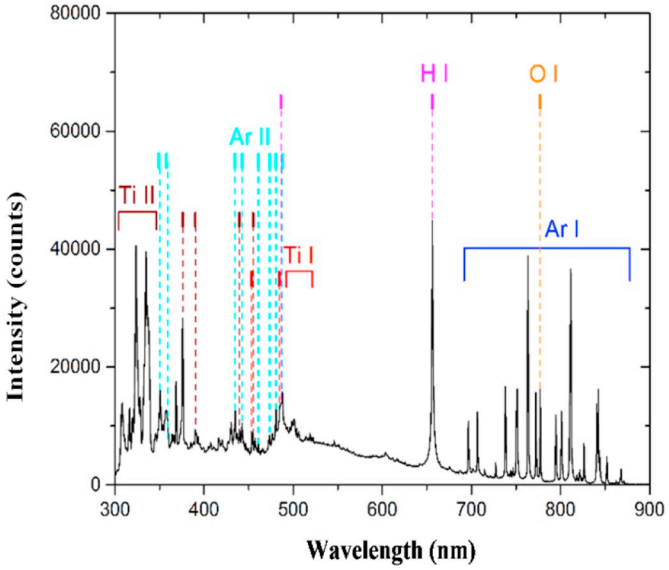


**Fig. 4.** Optical emission spectrum of plasma (black line) and identified lines (color) @ 90 Hz gas discharge frequency in argon, 100 µS conductivity and positive polarity.

### 3.4. Transmission electron microscopy results

Furthermore, to validate recovery test results, transmission electron microscopy analyses were conducted. As treatment by liquid phase plasma discharges in bubbles in argon showed complete inactivation of yeast cells, we have proposed the most effective treatment (90 Hz, 10 min, argon) for transmission electron microscopy analyses. Fig. 5a provides the results obtained before treatment where the cell wall and the plasma membrane are well-defined as the cellular organelles (nucleus, mitochondria, endoplasmic reticulum). Fig. 5b presents *S. cerevisiae* ATCC 204508 cells after the treatment by liquid phase plasma discharges in bubbles, where cell disintegration can be noted. Some of the cells are completely vacuolated with the inability to distinguish the organelles. Difference in cell wall and the cell membrane can't be detected. Furthermore, there are visible ruptures on the cell wall and the membrane, whereby a partial leakage of the cellular content into the surrounding medium occurs. Some of the cells are irreversibly permeabilized which resulted in complete leakage of intracellular

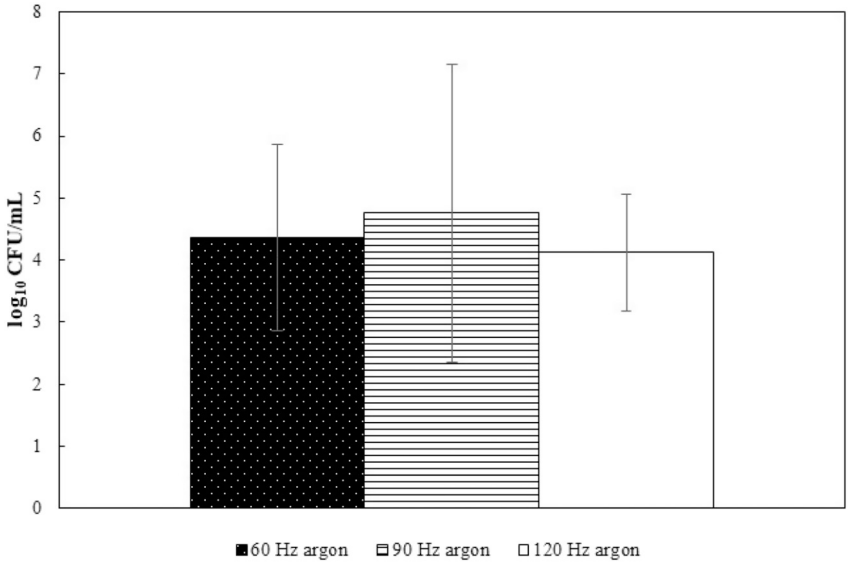


**Fig. 3.** The effect of frequency, time (10 min) and injected gas on recovery of *S. cerevisiae* ATCC 204508 after liquid phase plasma discharges in bubbles.

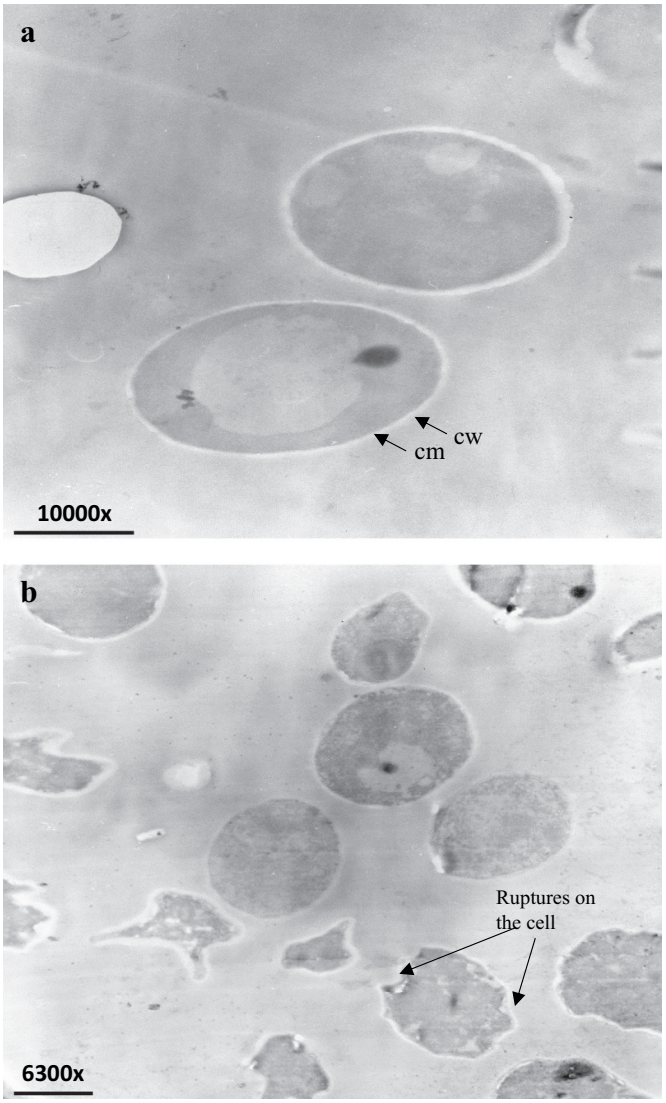


**Fig. 5.** Transmission electron microscopy figures of *S. cerevisiae* ATCC 204508 cells before (a) and after (b) the treatment by liquid phase plasma discharges in bubbles (90 Hz, 10 min, argon). cw-Cell wall, cm-cell membrane.

organelles. But, clearly there are still cells with intact cell wall, membrane and cellular macromolecules that can recover in optimal growth conditions.

### 3.5. Proteomic results of a single treated S. cerevisiae cells

Finally, to define response mechanisms of *S. cerevisiae* ATCC 204508 cells after the treatment (liquid phase plasma discharges in bubbles, 90 Hz, 10 min, argon), proteomic analyses were performed. Table 6 compares the proteins that are differentially expressed in non-treated and treated samples. Immediately after the treatment, treated cells overexpressed proteins that could be grouped into three broad categories: carbohydrate metabolism (glyceraldehyde-3-phosphate dehydrogenase 1, phosphoglycerate mutase 1, phosphoglycerate kinase and fructose-biphosphate aldolase and alcohol dehydrogenase 1), protein synthesis (eukaryotic translation initiation factor 5A-2 and 40S ribosomal protein S19-A), protein transport (heat shock proteins SSA1 and SSA2) and cell division (cofilin). Proteins that were down-regulated could be grouped in four groups: protein synthesis (elongation factor 1-beta, nascent polypeptide-associated complex subunit beta-1), cell cycle regulation (polyubiquitin), ribosome metabolism (ubiquitin-40S ribosomal protein S31, ubiquitin-60S ribosomal protein L40 and 60S acidic ribosomal protein P1-alpha) and stress response (superoxide dismutase [Mn], mitochondrial and peroxiredoxin).

### 3.6. Proteomic results of a recovered S. cerevisiae cells

Table 7 compares the proteins that are differentially expressed before and after the recovery test. Proteins overexpressed after the recovery were grouped in four categories: stress response (ubiquitin-like protein), protein synthesis (nascent polypeptide-associated complex subunit beta-1, 40S ribosomal protein S19-B and eukaryotic translation initiation factor 5A-2), cell homeostasis (adenylate kinase) and carbohydrate metabolism (enolase 2 and glyceraldehyde-3-phosphate dehydrogenase 1). Proteins down-regulated were grouped in: stress response (superoxide dismutase [Mn], mitochondrial, superoxide dismutase [Cu-Zn] and peroxiredoxin), protein synthesis (60S acidic ribosomal protein P1-beta, 40S ribosomal protein S17-B, 40S ribosomal protein S17-A and 60S acidic ribosomal protein P1-alpha), cell wall organization (protein ZEO1) and calcium ion binding (myosin light chain 1 and calmodulin).

### 3.7. Proteomic results of a three times treated S. cerevisiae cells

Table 8 presents the overview of the proteins that are differentially expressed in *S. cerevisiae* cells before and after the three times treatment of the same sample. After three times treatment overexpressed proteins were grouped in: synthesis of protein (nascent polypeptide-associated complex subunit beta-1, 60S ribosomal protein L19-B, 60S ribosomal protein L19-A, 40S ribosomal protein S19-B and 40S ribosomal protein S19-A), carbohydrate metabolism (triosephosphate isomerase), nucleotide metabolism (adenylate kinase) and cellular proliferation (WW protein). Proteins down-regulated were grouped in: stress response (superoxide dismutase [Mn], mitochondrial and thioredoxin-1), protein synthesis (60S acidic ribosomal protein P2-alpha, 40S ribosomal protein S21-B, 40S ribosomal protein S17-A and 40S ribosomal protein S17-B), carbohydrate metabolism (enolase 1, enolase 2, glyceraldehyde-3-phosphate dehydrogenase 1, phosphoglycerate mutase 1) and cell wall organization (protein ZEO1).

## 4. Discussion

This study offers important insight on the inactivation and stress response of *S. cerevisiae* ATCC 204508 cells. Inactivation of microorganisms is a fundamental factor to determine the effectiveness of certain technology. As mentioned in the results, liquid phase plasma discharges in bubbles with the injected gas argon showed the best inactivation results. There are several possible explanations for these results. With this type of the plasma reactor, discharges are generated in bubbles and in the surrounding fluid, thereby plasma area is increased, compared to one in the gas phase reactor (Kurahashi et al., 1997). The present findings seem to be consistent with the research of Kim et al. (2013). They have demonstrated that the cold plasma treatment induces higher inactivation of *E. coli* cells if treated by pulsed electrical discharges within bubbles. As shown in the Tables 2 and 3 increasing frequency and treatment time resulted in higher conductivity, while the values of pH were decreased. This finding supports previous researches of Baroch et al. (2008), Jiang et al. (2014) and Kurahashi et al. (1997). During the plasma treatment the increase in conductivity (from 12.2–68.6 μS/cm) is directly related to lower pH (Tables 3 and 4). It is therefore likely that during the plasma treatment in the gas phase, dissolution of the nitrogen oxide (Pavlovich et al., 2014; Sathiamoorthy et al., 1999) and formation of $H_3O^+$ ions due to electrostatic and ionic bombing of the water molecule occur (Hickling, 1971). Conductivity is also associated with the formation of hydrogen ions which directly binds the pH (Baroch et al., 2008), while $H_2O_2$ formation is directly related to OH· radicals in both, gas and liquid phase discharges (Kurahashi et al., 1997). Increased conductivity is also influenced by

**Table 6**
Overview of the changes in intracellular protein contents of *S. cerevisiae* ATCC 204508 cells before and after treatment by liquid phase plasma discharges in bubbles (90 Hz, 10 min, argon). Quantitative difference is shown as averaged PLGS ratios from two biological replicates for the treated cells with respect to the no treated cells. Probability of up or downregulation was ≥95%. Fold change cutoff was > 1.5 (see Section 2.7). Qualitative Protein only appeared in one condition (no treated or treated) and presents qualitative difference.

| Accession no. UniProt[a] | Protein name[b] | Gene[c] | Function[d] | Unique[e] | Ratio (treated:no treated)[f] | Log(e) variance (treated:no treated) |
|---|---|---|---|---|---|---|
| P32471 | Elongation factor 1-beta | EFB1 | Nucleotide metabolism | | 0.418951547 | 0.15 |
| Q02642 | Nascent polypeptide-associated complex subunit beta-1 | EGD1 | Translation | | 0.449328959 | 0.46 |
| P0CG63 | Polyubiquitin | UBI4 | DNA repair, cell cycle regulation | | 0.453844786 | 0.11 |
| P05759 | Ubiquitin-40S ribosomal protein S31 | RPS31 | Ribosome metabolism | | 0.458406024 | 0.15 |
| P0CH09 | Ubiquitin-60S ribosomal protein L40 | RPL40B | Ribosome metabolism | | 0.458406024 | 0.13 |
| P05318 | 60S acidic ribosomal protein P1-alpha | RPP1A | Ribosome metabolism | | 0.565525443 | 0.28 |
| P10592 | Heat shock protein SSA2 | SSA2 | ATPase activity, tRNA binding | | 1.584073998 | 0.09 |
| P10591 | Heat shock protein SSA1 | SSA1 | ATPase activity, tRNA binding, translation, stress granule disassembly | | 1.632316236 | 0.11 |
| P00360 | Glyceraldehyde-3-phosphate dehydrogenase 1 | TDH1 | Gluconeogenesis, glycolitic process, NAD and NADH binding | | 1.858928051 | 0.22 |
| P00950 | Phosphoglycerate mutase 1 | GMP1 | Pyruvate synthesis | | 1.22554095 | 0.13 |
| P00560 | Phosphoglycerate kinase | PGK1 | Pyruvate synthesis | | 1.993715528 | 0.19 |
| P00447 | Superoxide dismutase [Mn], mitochondrial | SOD2 | Destroys superoxide anion radicals | No treated | | |
| P38013 | Peroxiredoxin | AHP1 | Cell protection against oxidative stress | No treated | | |
| Q06146 | Uncharacterized protein | YRL257W | Unknown | No treated | | |
| P14540 | Fructose-biphosphate aldolase | FBA1 | Catalyzes reverse reaction in glycolysis | Treated | | |
| P00330 | Alcohol dehydrogenase 1 | ADH1 | Catalyzes the conversion of primary unbranched alcohols to their corresponding aldehydes | Treated | | |
| Q12138 | Putative uncharacterized protein | YRL125W | Unknown | Treated | | |
| Q03048 | Cofilin | COF1 | Cell division | Treated | | |
| P19211 | Eukaryotic translation initiation factor 5A-2 | ANB1 | Translation | Treated | | |
| P07280 | 40S ribosomal protein S19-A | RPS19A | Synthesis of proteins | Treated | | |

[a] Unique alphanumeric identifier of each entry in UniProt database.
[b] Full protein name recommended by the UniProt database consortium.
[c] Unique alphanumeric identifier used to represent the gene.
[d] Function(s) of a protein according to UniProt database.
[e] Protein only appeared in one condition (no treated or after 10 min 90 Hz treatment) and presents qualitative difference.
[f] Ratio of calculated relative abundance of treated and no treated sample. Ratio presents a relationship between treated and no treated samples, ratio > 0 indicates overexpression in treated cells and ratio < 0 indicates overexpression in no treated cells.

**Table 7**
Overview of the changes in intracellular protein contents of *S. cerevisiae* ATCC 204508 cells of non-treated cells and recovered cells. Quantitative difference is shown as averaged PLGS ratios from two biological replicates for the recovered cells with respect to the no treated cells. Probability of up or downregulation was ≥95%. Fold change cutoff was > 1.5 (see Section 2.7). Qualitative Protein only appeared in one condition (no treated or recovered) and presents qualitative difference.

| Accession no. UniProt[a] | Protein name[b] | Gene[c] | Function[d] | Unique[e] | Ratio (recovery:no treated)[f] | Log(e) variance (recovery:no treated) |
|---|---|---|---|---|---|---|
| P10622 | 60S acidic ribosomal protein P1-beta | RPP1B | Synthesis of proteins | | 0.199887611 | 0.12 |
| P14127 | 40S ribosomal protein S17-B | RPS17B | Synthesis of proteins | | 0.418951547 | 0.71 |
| Q08245 | Protein ZEO1 | ZEO1 | Cell wall organization | | 0.481908981 | 0.14 |
| P00445 | Superoxide dismutase [Cu-Zn] | SOD1 | Destroys radicals which are normally produced within the cells | | 0.419644208 | 0.07 |
| P02407 | 40S ribosomal protein S17-A | RPS17A | Synthesis of proteins | | 0.554327299 | 0.15 |
| P38013 | Peroxiredoxin | AHP1 | Cell redox homeostasis, response to oxidative stress | | 0.565525443 | 0.22 |
| P05318 | 60S acidic ribosomal protein P1-alpha | RPP1A | Synthesis of proteins | | 0.565525443 | 0.14 |
| P53141 | Myosin light chain 1 | MLC1 | Calcium ion binding, actomyosin contractile ring assembly | | 0.618783398 | 0.19 |
| P06787 | Calmodulin | CMD1 | Calcium ion binding, cell budding | | 0.657046828 | 0.1 |
| Q02642 | Nascent polypeptide-associated complex subunit beta-1 | EGD1 | Transcription, DNA-templated | | 1.537257535 | 0.2 |
| P00925 | Enolase 2 | ENO2 | Pyruvate synthesis | | 2.013752683 | 0.45 |
| P00360 | Glyceraldehyde-3-phosphate dehydrogenase 1 | TDH1 | Pyruvate synthesis | | 2.075080647 | 0.14 |
| P00447 | Superoxide dismutase [Mn], mitochondrial | SOD2 | Destroys superoxide anion radicals | No treated | | |
| Q12306 | Ubiquitin-like protein | SMT3 | Response to stress | Recovery | | |
| P07170 | Adenylate kinase | ADK1 | Cellular energy homeostasis and in adenine nucleotide metabolism | Recovery | | |
| P07281 | 40S Ribosomal protein S19-B | RPS19B | Synthesis of proteins | Recovery | | |
| P19211 | Eukaryotic translation initiation factor 5A-2 | ANB1 | Translation | Recovery | | |

[a] Unique alphanumeric identifier of each entry in UniProt database.
[b] Full protein name recommended by the UniProt database consortium.
[c] Unique alphanumeric identifier used to represent the gene.
[d] Function(s) of a protein according to UniProt database.
[e] Protein only appeared in one condition (no treated or 48 h recovery) and presents qualitative difference.
[f] Ratio of calculated relative abundance of recovered and no treated sample. Ratio presents a relationship between recovered and no treated samples, ratio > 0 indicates overexpression in recovered cells and ratio < 0 indicates overexpression in no treated cells.

**Table 8**
Overview of the changes in intracellular protein contents of *S. cerevisiae* ATCC 204508 cells before and after the three times treatment by liquid phase plasma discharges in bubbles (90 Hz, 10 min, argon). Quantitative difference is shown as averaged PLGS ratios from two biological replicates for the three times treated cells with respect to the no treated cells. Probability of up or downregulation was ≥95%. Fold change cutoff was > 1.5 (see Section 2.7). Qualitative Protein only appeared in one condition (no treated or three times treated) and presents qualitative difference.

| Accession no. UniProt[a] | Protein name[b] | Gene[c] | Function[d] | Unique[e] | Ratio (treated:no treated)[f] | Log(e) variance (treated:no treated) |
|---|---|---|---|---|---|---|
| P22217 | Thioredoxin-1 | TRX1 | Homeostasis, response to oxidative stress, glutathione metabolic process | | 0.138069235 | 0.35 |
| P00925 | Enolase 2 | ENO2 | Pyruvate synthesis | | 0.205975089 | 0.25 |
| P00924 | Enolase 1 | ENO1 | Pyruvate synthesis | | 0.26447725 | 0.34 |
| P00360 | Glyceraldehyde-3-phosphate dehydrogenase 1 | TDH1 | Pyruvate synthesis | | 0.280831627 | 0.23 |
| Q08245 | Protein ZEO1 | ZEO1 | Cell wall organization | | 0.332871076 | 0.18 |
| P00950 | Phosphoglycerate mutase 1 | GPM1 | Pyruvate synthesis | | 0.423162076 | 0.23 |
| P05319 | 60S acidic ribosomal protein P2-alpha | RPP2A | Translation | | 0.431710535 | 0.06 |
| Q3E754 | 40S ribosomal protein S21-B | RPS21B | Translation | | 0.472366553 | 0.07 |
| P33331 | Nuclear transport factor 2 | NTF2 | Nucleocytoplasmic transport | | 0.565525443 | 0.13 |
| P02407 | 40S ribosomal protein S17-A | RPS17A | Translation | | 0.612626388 | 0.19 |
| P14127 | 40S ribosomal protein S17-B | RPS17B | Translation | | 0.618783398 | 0.21 |
| Q02642 | Nascent polypeptide-associated complex subunit beta-1 | EGD1 | Regulation of transcription | | 1.786038401 | 0.54 |
| P00447 | Superoxide dismutase [Mn], mitochondrial | SOD2 | Destroys superoxide anion radicals | No treated | | |
| Q06146 | Uncharacterized protein | YRL257W | Growth protein | No treated | | |
| P00942 | Triosephosphate isomerase | TPI1 | Carbohydrate biosynthesis | 3× treated | | |
| P0CX83 | 60S Ribosomal protein L19-B | RPL19B | Translation | 3× treated | | |
| P0CX82 | 60S Ribosomal protein L19-A | RPL1A | Translation | 3× treated | | |
| P43582 | WW protein | WWM1 | Apoptosis, cellular proliferation | 3× treated | | |
| P07170 | Adenylate kinase | ADK1 | Cellular energy homeostasis, adenine nucleotide metabolism | 3× treated | | |
| P07281 | 40S Ribosomal protein S19-B | RPS19B | Translation | 3× treated | | |
| P07280 | 40S Ribosomal protein S19-A | RPS19A | Translation | 3× treated | | |

[a] Unique alphanumeric identifier of each entry in UniProt database.
[b] Full protein name recommended by the UniProt database consortium.
[c] Unique alphanumeric identifier used to represent the gene.
[d] Function(s) of a protein according to UniProt database.
[e] Protein only appeared in one condition (no treated or three times treated for 10 min 90 Hz) and presents qualitative difference.
[f] Ratio of calculated relative abundance of three times treated and no treated sample. Ratio presents a relationship between three times treated and no treated samples, ratio > 0 indicates overexpression in three times treated cells and ratio < 0 indicates overexpression in no treated cells.

the ions released from the cells into the surrounding medium during the treatment. Various studies have shown that lower pH (around 4) does not significantly affect bacterial inactivation while, yeast cells can survive at the pH below 2 (Korachi et al., 2010; Wheeler et al., 1991). In this paper, it is very unlikely that only pH has an effect on the inactivation of yeast cells while the lowest pH was around 4. On the other hand, probably the most significant inactivation mechanism in liquid phase discharges with the conductivity < 200 μS/cm is due to applied electric field and consequently electroporation processes (Vukusic et al., 2016).

As previously mentioned, during the plasma discharges different radical species can be formed as O·, $O_2$, $O_3$, OH·, $H_2O_2$ (Perni et al., 2008; Sharma et al., 2009), which can cause DNA (Cabiscol Català et al., 2000; Lu et al., 2014) and lipid oxidation of the cell (Gaunt et al., 2006; Mai-Prochnow et al., 2014). Despite the discharges in argon (argon ions and atoms are produced) which is an inert gas that inhibits the reaction of the generated radicals with the cellular molecules, nitrogen present in the air reacts with the oxygen and therefore reactive nitrogen radicals (RNS) are generated which can affect oxidation of the cell membrane. Discharges in the liquid phase in bubbles are major influenced by gas composition. Noble gases produce more volumetric discharges within the gas bubbles while oxygen affects the propagation along the gas-liquid interface (Tachibana et al., 2011).

In the samples where complete yeast cell inactivation's were observed (Fig. 2b.), recoveries of treated cells were high (around 5 $\log_{10}$ CFU/mL). This finding was unexpected and suggests that the cells were not inactivated, but in a special state called viable but non-culturable (VBNC). In that kind of state microorganisms fails to grow on selective media, have low metabolic activity, but are still alive (Oliver, 2010). Such cells exceed the decrease of macromolecular synthesis, but plasmids maintain the ATP level and high membrane potential (Oliver, 2010, p. 407).

According to the transmission electron microscopy images after the treatment some of the cells are characterized by intact cell wall and membrane, while some of the cells are completely inactivated with totally disintegrated membrane. During the plasma treatment generated radical species, electric filed and cavitation can influence the electroporation of the cell membrane (Liao et al., 2017; Locke et al., 2006). Because of the electropermeabilization, ruptures on the cell membrane and leakage of cell macromolecules can occur as shown on the transmission electron microscopy figures. Oxidizing radicals can find an easier entrance to the cells and cause different chemical reactions in the cytoplasm of the cell which leads to lethal damage of the cell.

The microorganism's cells react to stress factors through various adaptive mutations or production of defensive proteins. On the other hand, different protein interactions occur to achieve favorable conditions for the cell function. A comparative proteomic approach was employed to establish molecular response mechanisms of the cells immediately after the treatment by liquid phase plasma discharges in bubbles (90 Hz, 10 min, argon), after recovery test and after three times treatment. In Tables 6, 7 and 8 are listed the proteins that are found as differentially expressed.

Treated cells down-regulated proteins with functions: protein synthesis, cell cycle regulation, ribosome metabolism and stress response (Table 6). Interestingly, treated cells did not express superoxide

dismutase [Mn], mitochondrial and peroxiredoxin. Superoxide dismutase is responsible for destroying the superoxide anion radicals, which are normally produced within the cells and have a toxic influence on biological systems (Gaunt et al., 2006). Peroxiredoxin plays a very important role in the cellular protection against oxidative species. Catalyzes the reduction of hydrogen peroxide molecule on alcohol and water and is involved in $Mn^{2+}$ homeostasis (Archibald and Fridovich, 1982; McNaughton et al., 2010). Superoxide dismutase [Mn], mitochondrial and peroxiredoxin were not detected in treated cells comparing to non-treated cells, indicating that treatment trigger another defense mechanism against oxidative stress. In the study of Willi et al. (2018) is shown that oxidation stress can impair different steps in the ribosomal elongation cycle. Furthermore, it is proven that removal of damaged ribosomal components could allow the cell to repair faulty ribosomes (Mathis et al., 2017). We suppose that down-regulation of proteins involved in protein synthesis (elongation factor 1-beta, nascent polypeptide-associated complex subunit beta-1) and ribosome metabolism (ubiquitin-40S ribosomal protein S31, ubiquitin-60S ribosomal protein L40 and 60S acidic ribosomal protein P1-alpha) is important strategy in recovery process. Up-regulation of carbohydrate pathways indicates that energy is required to maintain defense against the stress in surrounding environment. Thorpe et al. (2004) showed that pentose phosphate pathway and control of the balance between glycolysis and gluconeogenesis were essential for *S. cerevisiae* resistance against oxidative stress caused by lipid peroxidation and superoxide-generating agent menadione. The changes in protein profiles upon exposure of *Paracoccidioides* yeast to $H_2O_2$ also showed increased expression of proteins involved in pentose phosphate pathway and gluconeogenesis (de Arruda Grossklaus et al., 2013). Our results suggest that the similar response mechanism is activated during liquid phase plasma treatment. Contrary, in proteomic study of *Candida* species to oxidative stress, it was found that TDH1 was downregulated in *C. parapsilosis* in the presence the menadione, and GMP1 was downregulated in *C. albicans* and *C. glabrata* in the presence of $H_2O_2$ indicating that mentioned response mechanism is species and stress type characteristic.

After the treatment, active defense *S. cerevisiae* accomplished through up-regulation of eukaryotic initiation translational factor 5A-2, heat shock proteins SSA1 and SSA2 and cofilin. Eukaryotic initiation translational factor 5A-2 is an essential protein involved in protein synthesis, cell proliferation, cell wall integrity preservation, and it reduces the translation process by reducing mRNA (Park, 2006). Recent evidence suggests that eIF5A may play a role in environmental adaptation and oxidative stress response (Pelechano and Alepuz, 2017). Our results strongly support this theory. Heat shock proteins SSA1 and SSA2 are chaperons with a role in the transport of polypeptides across the mitochondrial membranes into the endoplasmic reticulum (Li et al., 2003). Although SSA1 and SSA2 are heat shock proteins, published papers demonstrated that both SSA1 and SSA2 are up-regulated under oxidative stress in yeasts (Lee et al., 1999; Ramírez-Quijas et al., 2015), which is consistent with up-regulation of these proteins in cells after plasma treatment. The polarized growth of yeast cells after the treatment was catalyzed by a cofilin enzyme that employs polymerization of actin subunits and is overexpressed in an environment with higher concentration of oxidative species (Bernstein and Bamburg, 2010). Overexpression of cofilin strongly supports ability of the cells to recover after treatment.

Following 48 h recovery, differences in protein expression between treated and non-treated cells were still noticeable (Table 7). It can be seen that after recovery ANB1 was still strongly up-regulated. These results confirm its significance in cellular stress response to plasma treatment. After recovery, another protein associated with stress defense was up-regulated, SMT3. SMT3 is a small regulatory protein present in all eukaryotes. It has activity in various cellular processes such as response to stress and external factors, DNA transcription and its repair system (Hicke, 2001). However, proteins that protect the cells from oxidative stress were still down-regulated (SOD1, SOD2 and APH1). As SOD1 and APH1 were not detected immediately after the treatment (Table 6), these results suggest that cells ultimately started with protection against oxidative stress, but with delay. Ribosomal components (RPP1A, RPP1B, RPS17A and RPS17B) remained down-regulated indicating that recovery is still not complete. Proteins involved in carbohydrate pathways (ENO2 and TDH1) were up-regulated reflecting an increased consumption of glucose during recovery and leading to production of energy that was still required to maintain defense against remaining stress. Proteins involved in the budding process (MLC1 and CMD1) were down-regulated, but detected, indicating continuation of cellular proliferation after 48 h' recovery. The ADK1 overexpressed after the recovery analyses participates in the nucleotide metabolism (metabolism of purine bases) and cell homeostasis. It catalyzes the initiation of the DNA replication (Ma et al., 2010), which is another evidence of cell recovery after the treatment.

To gain an insight of the proteomic cellular responses during cells adaptation to plasma treatments we have also examined proteome changes that occurred after three times treatment of *S. cerevisiae* cells (Table 8). A similar protein expression was noticed for several proteins between cells that were treated three times and cells after recovery test (Table 7), including down-regulation of proteins with function in protein synthesis (RPS17A, RPS17A and RPP1A), cell wall organization (ZEO1) and with the function in maintaining of cellular redox homeostasis (SOD2). SOD2 was down-regulated immediately after the treatment (Table 6) and after recovery (Table 7). In three times treated cells, another protein involved in maintaining cellular redox homeostasis was down-regulated (TRX1). It seems that maintaining of cellular redox homeostasis is not essential for survival. The carbohydrate proteins (ENO1, ENO2, TDH1 and GPM1) were down-regulated in three times treatment, while after the single treatment (Table 6) and recovery test (Table 7) were overexpressed indicating that adaptive stress defense does not require additional energy to maintain defense against the stress. Similar indication was found in previous proteomic analysis of *S. saccharomyces* tolerant to phenol, furfural and acetic acid (PFA), where higher increase of important glycolysis enzymes was found in parental than in tolerant strain. Based on their results, the authors suggested that tolerant strain produces less energy to defend against PFA in comparison to parental strain (Ding et al., 2012). It is quite interesting that after three times treatment cells overexpressed a protein WWM1. WWM1 causes impaired growth when is overexpressed, but on the other hand, maintains the homeostasis of the cell (Stevenson et al., 2001). Its expression represents a widespread adaptation to osmotic stress (Szallies et al., 2002). These results suggest that the defense mechanism after three times treatment highlights the fact that cells were able to adapt to the plasma treatments.

## 5. Conclusions

This study was designed to determine the effect of gas phase and liquid phase plasma discharges in bubbles on the inactivation and stress response of *S. cerevisiae* ATCC 204508 cells. Based on the discussion above, it can be concluded that the liquid phase plasma discharges in bubbles in argon with a longer treatment time (10 min) at all applied frequencies (60, 90 and 120 Hz) led to higher inactivation results compared to gas phase plasma treatments. Although some of the treatments resulted in complete inactivation, transmission electron microscopy analyses showed that not all of the cells were lethally injured which consequently led to cell recovery. Proteomic analyses implied that *S. cerevisiae* cells activate defense mechanisms to overcome the stress conditions. This research has thrown up many questions in need of further investigation to define the optimum inactivation conditions which will disable cell recovery.

## Acknowledgements

The authors would like to acknowledge the support of the Croatian

Science Foundation and the project (HRZZ-IP-11-2013) “Application of electrical discharge plasma for preservation of liquid foods” and project “Equipping the semi-industrial practice for the development of new food technologies” (KK.01.1.1.02.0001).

## Conflict of interest

The authors declare no conflict of interest.

## Annex A

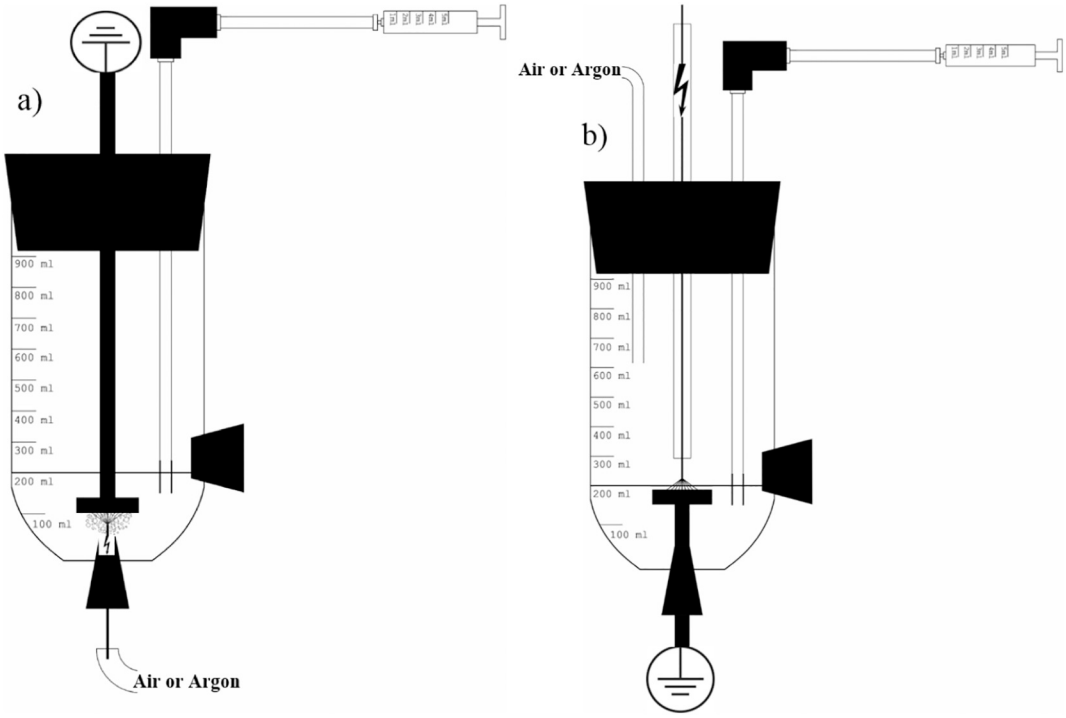


**Fig. A.1.** Schematic description of plasma reactor: liquid in a bubbles (a) and gas phase (b).

## References

Archibald, F.S., Fridovich, I., 1982. The scavenging of superoxide radical by manganous complexes: in vitro. Arch. Biochem. Biophys. 214, 452–463.
Baroch, P., Saito, N., Takai, O., 2008. Special type of plasma dielectric barrier discharge reactor for direct ozonization of water and degradation of organic pollution. J. Phys. D. Appl. Phys. 41, 085207.
Bernstein, B.W., Bamburg, J.R., 2010. ADF/cofilin: a functional node in cell biology. Trends Cell Biol. 20, 187–195.
Cabiscol Català, E., Tamarit Sumalla, J., Ros Salvador, J., 2000. Oxidative stress in bacteria and protein damage by reactive oxygen species. Int. Microbiol. 3, 3–8.
de Arruda Grossklaus, D., Bailão, A.M., Rezende, T.C.V., Borges, C.L., de Oliveira, M.A.P., Parente, J.A., de Almeida Soares, C.M., 2013. Response to oxidative stress in *Paracoccidioides* yeast cells as determined by proteomic analysis. Microbes Infect. 15, 347–364.
Ding, M.Z., Wang, X., Liu, W., Cheng, J.S., Yang, Y., Yuan, Y.J., 2012. Proteomic research reveals the stress response and detoxification of yeast to combined inhibitors. PLoS One 7, e43474.
Eisenberg, G., 1943. Colorimetric determination of hydrogen peroxide. Ind. Eng. Chem. Anal. Ed. 15, 327–328.
Fridman, G., Brooks, A.D., Balasubramanian, M., Fridman, A., Gutsol, A., Vasilets, V.N., Aylan, H., Friedman, G., 2007. Comparison of direct and indirect effects of non-thermal atmospheric-pressure plasma on bacteria. Plasma Process. Polym. 4, 370–375.
Gaunt, L.F., Beggs, C.B., Georghiou, G.E., 2006. Bactericidal action of the reactive species produced by gas-discharge nonthermal plasma at atmospheric pressure: a review. IEEE Trans. Plasma Sci. 34, 1257–1269.
Griem, H.R., 1974. Spectral Line Broadening by Plasmas, first ed. Academic Press, New York.
Hicke, L., 2001. Ubiquitin and proteasomes: protein regulation by monoubiquitin. Nat. Rev. Mol. Cell Biol. 2, 195.
Hickling, A., 1971. Electrochemical Processes in Glow Discharge at the Gas-Solution Interface, first ed. Springer, Boston.
Inagaki, N., 1996. Plasma Surface Modification and Plasma Polymerization, first ed. CRC Press, Boca Raton.
Jiang, B., Zheng, J., Qiu, S., Wu, M., Zhang, Q., Yan, Z., Xue, Q., 2014. Review on electrical discharge plasma technology for wastewater remediation. Chem. Eng. J. 236, 348–368.
Kim, H.S., Cho, Y.I., Hwang, I.H., Lee, D.H., Cho, D.J., Rabinovich, A., Fridman, A., 2013. Use of plasma gliding arc discharges on the inactivation of *E. coli* in water. Sep. Purif. Technol. 120, 423–428.
Korachi, M., Turan, Z., Şentürk, K., Şahin, F., Aslan, N., 2009. An investigation into the biocidal effect of high voltage AC/DC atmospheric corona discharges on bacteria, yeasts, fungi and algae. J. Electrost. 67, 678–685.
Korachi, M., Gurol, C., Aslan, N., 2010. Atmospheric plasma discharge sterilization effects on whole cell fatty acid profiles of *Escherichia coli* and *Staphylococcus aureus*. J. Electrost. 68, 508–512.
Kurahashi, M., Katsura, S., Mizuno, A., 1997. Radical formation due to discharge inside bubble in liquid. J. Electrost. 42, 93–105.
Lee, J., Godon, C., Lagniel, G., Spector, D., Garin, J., Labarre, J., Toledano, M.B., 1999. Yap1 and Skn7 control two specialized oxidative stress response regulons in yeast. J. Biol. Chem. 274, 16040–16046.
Li, X.S., Reddy, M.S., Baev, D., Edgerton, M., 2003. *Candida albicans* Ssa1/2 is the cell envelope binding protein for human salivary Histatin 5. J. Biol. Chem. 278, 28553–28561.
Liao, X., Liu, D., Xiang, Q., Ahn, J., Chen, S., Ye, X., Ding, T., 2017. Inactivation mechanisms of non-thermal plasma on microbes: a review. Food Control 75, 83–91.
Locke, B.R., Sato, M., Sunka, P., Hoffmann, M.R., Chang, J.S., 2006. Electrohydraulic discharge and nonthermal plasma for water treatment. Ind. Eng. Chem. Res. 45, 882–905.
Lu, H., Patil, S., Keener, K.M., Cullen, P.J., Bourke, P., 2014. Bacterial inactivation by high-voltage atmospheric cold plasma: influence of process parameters and effects on cell leakage and DNA. J. Appl. Microbiol. 116, 784–794.
Lu, X., Naidis, G.V., Laroussi, M., Reuter, S., Graves, D.B., Ostrikov, K., 2016. Reactive species in non-equilibrium atmospheric-pressure plasmas: generation, transport, and biological effects. Phys. Rep. 630, 1–84.
Ma, L., Zhai, Y., Feng, D., Chan, T.C., Lu, Y., Fu, X., Wang, J., Chen, Y., Li, J., Xu, K., Liang, C., 2010. Identification of novel factors involved in or regulating initiation of DNA replication by a genome-wide phenotypic screen in *Saccharomyces cerevisiae*. Cell Cycle 9, 4399–4410.
Mai-Prochnow, A., Murphy, A.B., McLean, K.M., Kong, M.G., Ostrikov, K.K., 2014. Atmospheric pressure plasmas: infection control and bacterial responses. Int. J. Antimicrob. Agents 43, 508–517.
Mathis, A.D., Naylor, B.C., Carson, R.H., Evans, E., Harwell, J., Knecht, J., ... Transtrum, M.K., 2017. Mechanisms of in vivo ribosome maintenance change in response to

nutrient signals. Mol. Cell. Proteomics 16 (2), 243–254.
McNaughton, R.L., Reddi, A.R., Clement, M.H., Sharma, A., Barnese, K., Rosenfeld, L., Gralla, E.D., Valentine, J.S., Cullota, V.C., Hoffman, B.M., 2010. Probing in vivo $Mn^{2+}$ speciation and oxidative stress resistance in yeast cells with electron-nuclear double resonance spectroscopy. Proc. Natl. Acad. Sci. 107, 15335–15339.
Misra, N.N., Tiwari, B.K., Raghavarao, K.S.M.S., Cullen, P.J., 2011. Nonthermal plasma inactivation of food-borne pathogens. Food Eng. Rev. 3, 159–170.
Moreau, M., Orange, N., Feuilloley, M.G.J., 2008. Non-thermal plasma technologies: new tools for bio-decontamination. Biotechnol. Adv. 26, 610–617.
Oberg, A.L., Vitek, O., 2009. Statistical design of quantitative mass spectrometry-based proteomic experiments. J. Proteome Res. 8, 2144–2156.
Oliver, J.D., 2010. Recent findings on the viable but nonculturable state in pathogenic bacteria. FEMS Microbiol. Rev. 34, 415–425.
Park, M.H., 2006. The post-translational synthesis of a polyamine-derived amino acid, hypusine, in the eukaryotic translation initiation factor 5A (eIF5A). J. Biochem. 139, 161–169.
Pavlovich, M.J., Clark, D.S., Graves, D.B., 2014. Quantification of air plasma chemistry for surface disinfection. Plasma Sources Sci. Technol. 23, 065036.
Pelechano, V., Alepuz, P., 2017. eIF5A facilitates translation termination globally and promotes the elongation of many non polyproline-specific tripeptide sequences. Nucleic Acids Res. 45, 7326–7338.
Perni, S., Shama, G., Kong, M.G., 2008. Cold atmospheric plasma decontamination of the pericarps of fruit. J. Food Prot. 71, 302–308.
Ramírez-Quijas, M.D., López-Romero, E., Cuéllar-Cruz, M., 2015. Proteomic analysis of cell wall in four pathogenic species of *Candida* exposed to oxidative stress. Microb. Pathog. 87, 1–12.
Sathiamoorthy, G., Kalyana, S., Finney, W.C., Clark, R.J., Locke, B.R., 1999. Chemical reaction kinetics and reactor modeling of $NO_x$ removal in a pulsed streamer corona discharge reactor. Ind. Eng. Chem. Res. 38, 1844–1855.
Sato, M., Ohgiyama, T., Clements, J.S., 1996. Formation of chemical species and their effects on microorganisms using a pulsed high-voltage discharge in water. IEEE Trans. Ind. Appl. 32, 106–112.
Scholtz, V., Pazlarova, J., Souskova, H., Khun, J., Julak, J., 2015. Nonthermal plasma—a tool for decontamination and disinfection. Biotechnol. Adv. 33, 1108–1119.
Sharma, A., Collins, G., Pruden, A., 2009. Differential gene expression in *Escherichia coli* following exposure to nonthermal atmospheric pressure plasma. J. Appl. Microbiol. 107, 1440–1449.
Stevenson, L.F., Kennedy, B.K., Harlow, E., 2001. A large-scale overexpression screen in *Saccharomyces cerevisiae* identifies previously uncharacterized cell cycle genes. Proc. Natl. Acad. Sci. 98, 3946–3951.
Szallies, A., Kubata, B.K., Duszenko, M., 2002. A metacaspase of *Trypanosoma brucei* causes loss of respiration competence and clonal death in the yeast *Saccharomyces cerevisiae*. FEBS Lett. 517, 144–150.
Tachibana, K., Takekata, Y., Mizumoto, Y., Motomura, H., Jinno, M., 2011. Analysis of a pulsed discharge within single bubbles in water under synchronized conditions. Plasma Sources Sci. Technol. 20, 034005.
Thorpe, G.W., Fong, C.S., Alic, N., Higgins, V.J., Dawes, I.W., 2004. Cells have distinct mechanisms to maintain protection against different reactive oxygen species: oxidative-stress-response genes. Proc. Natl. Acad. Sci. 101, 6564–6569.
Vukusic, T., Shi, M., Herceg, Z., Rogers, S., Estifaee, P., Thagard, S.M., 2016. Liquid-phase electrical discharge plasmas with a silver electrode for inactivation of a pure culture of *Escherichia coli* in water. Innov. Food Sci. Emerg. Technol. 38, 407–413.
Walker, G.M., 1998. Yeast Physiology and Biotechnology, first ed. John Wiley & Sons, New York.
Wheeler, K.A., Hurdman, B.F., Pitt, J.I., 1991. Influence of pH on the growth of some toxigenic species of *Aspergillus*, *Penicillium* and *Fusarium*. Int. J. Food Microbiol. 12, 141–149.
Willi, J., Küpfer, P., Evéquoz, D., Fernandez, G., Katz, A., Leumann, C., Polacek, N., 2018. Oxidative stress damages rRNA inside the ribosome and differentially affects the catalytic center. Nucleic Acids Res. 46, 1945–1957.
Yu, H., Perni, S., Shi, J.J., Wang, D.Z., Kong, M.G., Shama, G., 2006. Effects of cell surface loading and phase of growth in cold atmospheric gas plasma inactivation of *Escherichia coli* K12. J. Appl. Microbiol. 101, 1323–1330.